

Ab Initio Study of the Hydrolysis Reactions of Neutral and Anionic Mg–Pyrophosphate Complexes in the Gas Phase

Humberto Saint-Martin^{*,†} and Luis E. Vicent^{†,‡}

Centro de Ciencias Físicas, Universidad Nacional Autónoma de México, Apartado Postal 48-3, Cuernavaca, Morelos 62251, México, and Facultad de Ciencias, Universidad Autónoma del Estado de Morelos, Cuernavaca, Morelos 62270, México

Received: May 14, 1999

Ab initio calculations were performed to study the stability of various anhydrous and monohydrated complexes of Mg^{2+} with pyrophosphates and orthophosphates at the self-consistent-field (SCF) and second-order perturbation (MP2) levels of the theory, using a 6-31+G** basis set with diffuse and polarization functions. New equilibrium geometries were found for the anhydrous Mg–pyrophosphate complexes, that modify previous estimates of the isomerization energies. It is found that the interaction with the water molecule stabilizes the pyrophosphates with respect to the metaphosphate-containing complexes, thus modifying the reaction energies to such an extent that the isomerization results are endothermic and nonspontaneous for the dianionic complex. However, the hydrolysis reactions are all exothermic and spontaneous. Moreover, it is found that the water molecule readily breaks upon interacting with the dianionic complex, producing a hydroxide anion: $\text{H}_2\text{O} + [\text{Mg}\cdot\text{P}_2\text{O}_7]^{2-} \rightarrow [\text{HO}\cdot\text{Mg}\cdot\text{HP}_2\text{O}_7]^{2-}$, and the resulting dianionic complex is much more stable than the isomer with a metaphosphate. It is shown that this result is consistent with both an associative and a dissociative mechanism for the hydrolysis. Finally, the estimate of free energies of solvation by means of the polarizable continuum model (PCM) yield values for the free energies of hydrolysis that are close to the experimental data.

1. Introduction

A central problem in biochemistry is the understanding of how enzymes work;¹ a proposed general mechanism is the principle of the transition-state stabilization, which asserts that an enzyme binds the reactants in their transition state with a higher affinity than it binds them in their ground state.² It is thus quite relevant to find the pathways corresponding to the biochemical reactions. The most ubiquitous reaction in metabolic processes is the hydrolysis of phosphoanhydride bonds,¹ and the simplest compound with such bonds is the diphosphoric acid, which is both biologically relevant^{3–5} and amenable to theoretical calculations.^{6–8} Furthermore, there is compelling evidence^{9–13} that the biologically active pyrophosphate species is the hydrated complex with magnesium $[\text{Mg}\cdot(\text{H}_2\text{O})_4\cdot\text{P}_2\text{O}_7]^{2-}$. This evidence is based on the analysis of the complexes that are present in the solution under physiological conditions.

The Mg–pyrophosphate complexes have been treated theoretically and a mechanism of hydrolysis was proposed by Ma et al.¹⁴ that involves the isomerization $\text{Mg}\cdot\text{H}_2\text{P}_2\text{O}_7 \rightarrow \text{PO}_3\cdot\text{Mg}\cdot\text{H}_2\text{PO}_4$ as an intermediate step. This mechanism was further extended¹⁵ to the anionic complexes $[\text{Mg}\cdot\text{HP}_2\text{O}_7]^-$ and $[\text{Mg}\cdot\text{P}_2\text{O}_7]^{2-}$. These theoretical calculations correspond to the anhydrous gas phase and thus are lacking the effects of the interaction with the solvent, which have been argued to contribute to both the energy of the reaction and the activation barrier.^{16–18} Even though the microenvironment at the active sites of enzymes is presumably different from that of the aqueous

solution,^{19,20} a high-resolution X-ray experiment showed the presence of a substantial amount of water molecules²¹ making an intricate array of hydrogen bonds with the residues within the active site of the pyrophosphatase from the budding yeast *Saccharomyces cerevisiae*. In this experiment, a total of four cations was found within the active site, which leads to the proposal of an alternative mechanism, that considers the neutral $\text{Mg}_2\cdot(\text{H}_2\text{O})_8\cdot\text{P}_2\text{O}_7$ complex as the true substrate. According to this mechanism, hydrogen bonding and cation coordination play a major role, allowing the dissociation of one water molecule into a proton and the nucleophilic hydroxide anion that ultimately attacks one of the phosphorus atoms. Recent theoretical studies of pyrophosphate complexed to calcium²² and to zinc²³ support the relevance of the coordination properties of the metal cation. Such a complex scheme of interactions cannot be properly described with simple solvation models, so to gain insight into the combined role of hydrogen bonding and coordination properties it is necessary to study the interactions with explicit water molecules. Therefore, in the present work we decided to explore the equilibria among various isomers of the monohydrated complexes to test the possibility of dissociation of the water molecule and to study the effects of the interaction on the energetics and the mechanism of the hydrolysis reactions.

2. Computational Details

The GAUSSIAN-94/DFT²⁴ program was employed to perform ab initio calculations with its standard 6-31+G** basis set.²⁵ Though this basis set is not yet saturated, it was shown to yield reliable results for the Mg–pyrophosphate complexes in previous works.¹⁵

* Author to whom correspondence should be addressed. E-mail: humberto@fis.unam.mx.

† Universidad Nacional Autónoma de México.

‡ Universidad Autónoma del Estado de Morelos.

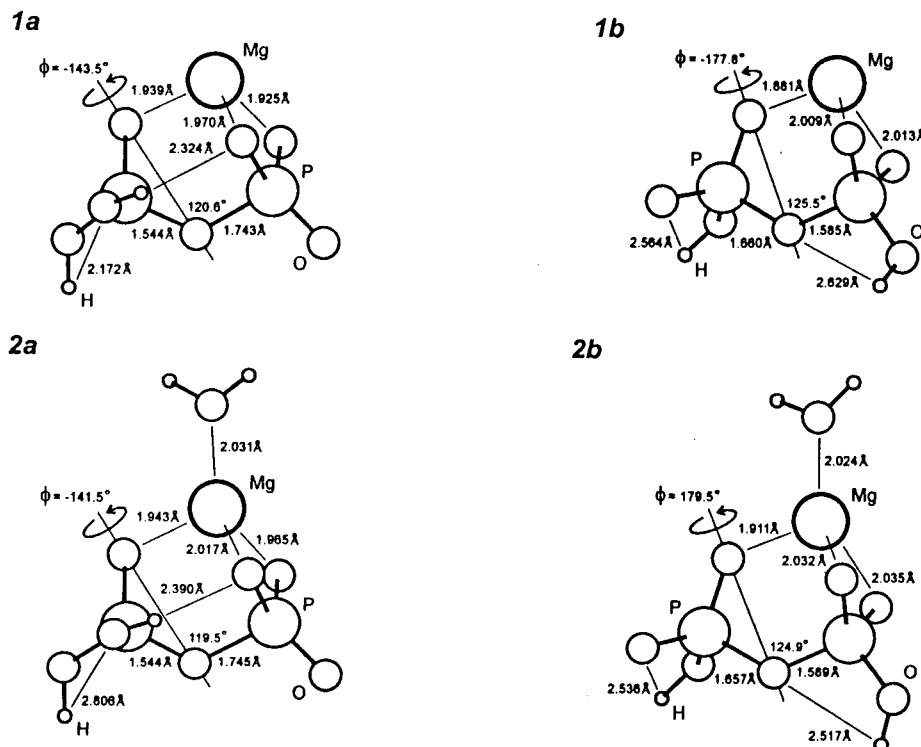


Figure 1. Anhydrous and monohydrated neutral $\text{Mg}\cdot\text{H}_2\text{P}_2\text{O}_7$ complex with the two protons at the orthophosphate moiety (**1a**, **2a**) and with one proton at each moiety (**1b**, **2b**). All have asymmetric P–O bonds, and the interaction with water produces little distortion. The lowest vibrational frequencies of all correspond to the bent of the orthophosphate with respect to the dihedral angle ϕ .

Geometry optimizations were performed at the SCF/6-31+G** level of the theory for all the molecular species studied. The corresponding analyses showed all the frequencies to be real, so the geometries found are all located at local minima in their respective energy surfaces.

The estimates of the energies ΔE_e^{SCF} of the isomerizations were computed with the SCF/6-31+G** optimized geometries, and the correlation energy was computed at the MP2/6-31+G** level. The calculation of the enthalpies included a term $\Delta E_{\text{th}}^{298}$ with the zero-point energy, *ZPE*, and the thermal vibrational energy at $T = 298.15$ K, both computed with a harmonic approximation:²⁵

$$\Delta H^\circ = \Delta E_e^{\text{SCF}} + \Delta E_e^{\text{MP2}} + \Delta E_{\text{th}}^{298} \quad (1)$$

The reference state is at $P = 0.1$ MPa. The vibrational entropies were also computed with a harmonic approximation and a canonical partition function, and summed to the translational, the rotational, and the electronic entropies according to standard statistical mechanics relationships.²⁵ The free energies were computed as the difference:

$$\Delta G = \Delta H - T\Delta S \quad (2)$$

To study the deformation induced by the interaction with the water molecule on the Mg–pyrophosphate complexes, the structural variations were quantified with the root-mean-square differences (RMS) of their coordinates, referred to their respective principal-moments-of-inertia frame.

3. Results

In the discussion of the structures depicted in Figures 1–6, we will refer to the leftmost phosphorus with the three nonbridging oxygens bonded to it and the bridging oxygen as the orthophosphate moiety, and to the rightmost phosphorus with

its respective three nonbridging oxygens as the metaphosphate moiety. Also, the abbreviation “Mg–PPi” will be used for the magnesium–pyrophosphate complex.

3.1. Hydrolysis of the Neutral Complex $\text{Mg}\cdot\text{H}_2\text{P}_2\text{O}_7$. 3.1.1.

Interaction of $\text{Mg}\cdot\text{H}_2\text{P}_2\text{O}_7$ with One Water Molecule. The optimum geometry found in previous works^{14,15,22} for the neutral anhydrous Mg–PPi complex is the staggered configuration **1a**, with the two protons at the orthophosphate moiety (Figure 1); the Mg^{2+} cation coordinates three oxygens: one from the orthophosphate moiety and two from the metaphosphate moiety, and a weak hydrogen bond is formed between one proton of the orthophosphate and an oxygen of the metaphosphate. The P–O bond from the orthophosphate to the bridging oxygen is shorter than the analogous bond with the metaphosphate. In this work a further search was performed, starting from various eclipsed configurations with four oxygens coordinated by the Mg^{2+} cation. A new stationary point was found (structure **1b**), that has a lower energy with respect to structure **1a**, $\Delta E^{\text{SCF}} = -16.7$ kJ/mol. Despite the initial eclipsed geometry, this new structure is staggered with only three oxygens coordinated by the Mg^{2+} cation, but with the protons placed at opposite moieties. The asymmetry of the electrostatic interactions induced by the cation produces the elongation of the bridging P–O bond with the orthophosphate, with respect to the other. The isomerization **1a** \rightarrow **1b** has an enthalpy of $\Delta H^\circ = -2.6$ kJ/mol and a free energy of $\Delta G^\circ = -6.4$ kJ/mol; because these values are in the limits of accuracy of the method, the theoretical prediction is that both structures are isoenergetic. It is also worth noticing that the difference in the bridging P–O bond lengths is smaller in structure **1b** ($\Delta r = 0.075$ Å compared to $\Delta r = 0.199$ Å in structure **1a**). Because the proposal of the reaction mechanism through a metaphosphate intermediate was based on the activation produced by the metal cation on the longest bridging P–O bond, we decided to make an analysis of the normal vibration modes of both structures **1a** and **1b** (Table 1). In both

TABLE 1: Lowest Vibrational Frequencies of Mg–Pyrophosphate Complexes^a

mode	1a	1b	2a	2b	6b	7	11a	11b	12a	12b
bending	99	54	114	63	99	136	47	193 ^b	43	149
B-S-J ^c	158	146		145	148	157	129		129	

^a All frequencies are in cm⁻¹. The numbers in bold face of the first row correspond to the structures depicted in Figures 1–6. ^b This bent is with respect to an axis passing through the Mg²⁺ cation and the bridging oxygen, whereas all others are respective to axes passing through the bridging oxygen and one oxygen coordinated by the cation. ^c B-S-J refers to the ball-and-socket joint motion described in the text.

TABLE 2: Interaction Energies, Enthalpies, Entropies, and Free Energies of Mg–Phosphates with One Water Molecule^a

interaction	ΔE_e^{SCF}	ΔE_e^{MP2}	$\Delta E_{\text{th}}^{298}$	ΔH°	ΔS°	ΔG°
1a + H ₂ O → 2a	-144.9	-3.8	9.7	-138.9	-113.7	-105.0
1b + H ₂ O → 2b	-147.2	-4.0	7.1	-144.1	-105.5	-112.6
3 + H ₂ O → 4a	-93.2	0.5	9.8	-82.9	-128.1	-44.7
3 + H ₂ O → 4b	-88.8	-10.6	9.7	-89.6	-126.9	-51.8
6b + H ₂ O → 7	-116.4	-9.5	10.7	-115.2	-133.0	-75.6
6b + OH ⁻ → 12b ^b	-218.3	10.5	9.0	-198.8	-124.3	-161.7
8 + H ₂ O → 9	-89.2	-1.6	11.0	-79.8	-130.6	-40.8
11a + H ₂ O → 12a	-113.9	-17.2	9.4	-121.7	-134.9	-81.5
8 + OH ⁻ → 14b ^b	-87.3	15.7	4.6	-67.0	-96.8	-38.1
11b + H ₂ O → 12b ^c	-365.1	21.7	8.9	-334.5	-136.7	-293.7
13a + H ₂ O → 14a	-94.3	-24.3	7.1	-111.5	-112.5	-78.0
13b + H ₂ O → 14b ^c	-264.4	7.2	4.1	-253.1	-134.4	-213.0

^a All energies and enthalpies are in kJ/mol. Entropies are in J/(mol K). ^b Interactions of monoanionic Mg–phosphates with a hydroxide anion. ^c In these reactions the water molecule releases a proton to the phosphate and the resulting hydroxide anion remains coordinated by the metal cation.

cases the lowest frequency corresponded to the bending of the dihedral between the plane defined by the phosphorus in the orthophosphate, its oxygen coordinated by the metal cation and the bridging oxygen, and the plane defined by the phosphorus in the metaphosphate, the metal cation, and the bridging oxygen (the dihedral ϕ depicted in Figure 1). The next frequency corresponded to the back-and-forth motion of the bridging

oxygen, relative to the plane defined by the cation and the phosphorus atoms, correlated to the rotation of the phosphate moieties around the axis passing through the P atoms. Thus, the reaction coordinate for the demise of one P–O bond is not its simple elongation,^{14,15} but rather the ball-and-socket joint motion proposed previously.¹⁶ Consequently, the activation barrier is likely to be smaller than the value reported in the literature,¹⁵ $\Delta G^\ddagger = 23.4$ kJ/mol.

In view of this situation, we decided to explore the equilibria of structures **1a** and **1b** in their interactions with one water molecule; thus both were used as starting points for the optimization of the H₂O·Mg·H₂P₂O₇ complex. The corresponding optimized geometries are structures **2a** and **2b** (Figure 1). The interaction with water, computed from H₂O + Mg·H₂P₂O₇ → H₂O·Mg·H₂P₂O₇, is quite strong in both cases (see Table 2), a little more for structure **2b**. However, the RMS difference (0.034 Å between **1a** and **2a**, and 0.093 Å between **1b** and **2b**) shows very little distortion of the Mg·H₂P₂O₇ complex. As it was found in recent works,^{22,23} the arrangement of oxygens coordinated by the cation corresponds to its first hydration shell.²⁶ In both cases, the lowest vibration frequencies are increased in more than 15%, indicating a stabilization with respect to the anhydrous species. Moreover, the ball-and-socket joint motion disappears in structure **2a**, whereas it remains unchanged in **2b**.

To better characterize the effect produced on the Mg·H₂P₂O₇ complex by the interaction with the water molecule, it is worth analyzing the charge distribution on the complexes. We chose to perform this in two different ways: by means of charges obtained from Mulliken population analysis,^{25,29} and by means of charges derived from the electrostatic potential within the CHELP scheme.³⁰ It should be kept in mind that all population analysis schemes are somewhat arbitrary, so the conclusions drawn from them are only qualitative. The charges on all atoms are available upon request to the authors.³¹ In Table 3 we concentrate on the Mg cation, the water molecule, the ortho-

TABLE 3: Charges on the Various Moieties of Mg–Phosphates and Solvation Free Energies Computed with PCM^{33 a}

structure	Mg	H ₂ O	ortho ^b	meta ^b	ΔG_{sol}^c
1a	0.99 (1.67)		-0.54 (-0.51)	-0.45 (-1.16)	-334.2
1b	0.97 (1.73)		-1.29 (-1.32)	0.32 (-0.41)	-348.5
2a	0.93 (1.66)	0.13 (0.01)	-0.59 (-0.51)	-0.46 (-1.16)	-314.7
2b	0.92 (1.60)	0.13 (0.04)	-1.39 (-1.29)	0.35 (-0.36)	-309.3
3	0.77 (1.65)		-0.32 (-0.81)	-0.45 (-0.84)	-281.9
4a	0.85 (1.65)	0.12 (-0.06)	-0.28 (-0.77)	-0.69 (-0.82)	-268.3
4b	0.72 (1.55)	0.11 (0.01)	-0.37 (-0.77)	-0.47 (-0.80)	-274.9
5	0.66 (1.45)				-284.6
6b	0.88 (1.65)		-1.38 (-1.42)	-0.50 (-1.24)	-490.7
7	0.83 (1.68)	0.14 (0.00)	-1.45 (-1.36)	-0.51 (-1.32)	-502.2
8	0.76 (1.65)		-1.21 (-1.74)	-0.55 (-0.91)	-459.2
9	0.84 (1.69)	0.12 (-0.06)	-1.21 (-1.70)	-0.74 (-0.93)	-474.8
10	0.63 (1.46)				-479.7
11a	0.77 (1.68)		-2.01 (-2.45)	-0.76 (-1.23)	-1101.7
11b	0.49 (1.64)		-1.92 (-2.27)	-0.57 (-1.37)	-1059.9
12a	0.67 (1.72)	0.17 (-0.05)	-2.09 (-2.33)	-0.74 (-1.34)	-1059.2
13a	1.00 (1.67)		-2.19 (-2.71)	-0.81 (-0.96)	-1045.5
13b	0.83 (1.60)		-2.06 (-2.68)	-0.77 (-0.92)	-1090.4
14a	0.88 (1.70)	0.09 (-0.06)	-2.17 (-2.65)	-0.80 (-0.99)	-989.8

structure	Mg	OH ^d	ortho	meta	ΔG_{sol}
12b	0.88 (1.75)	-0.70 (-0.97)	-1.53 (-1.43)	-0.06 (-0.49)	-963.4
14b	0.86 (1.80)	-0.72 (-0.95)	-1.13 (-1.86)	-1.01 (-0.99)	-962.7
15	0.68 (1.69)				-985.4

^a The charges are in atomic units and were obtained from Mulliken's population analysis; numbers in parentheses were obtained with the CHELP scheme. ^b Ortho refers to the orthophosphate moiety and meta to the metaphosphate moiety. ^c The solvation free energies are in kJ/mol. ^d In structures **12b** and **14b** there is a hydroxide anion instead of water.

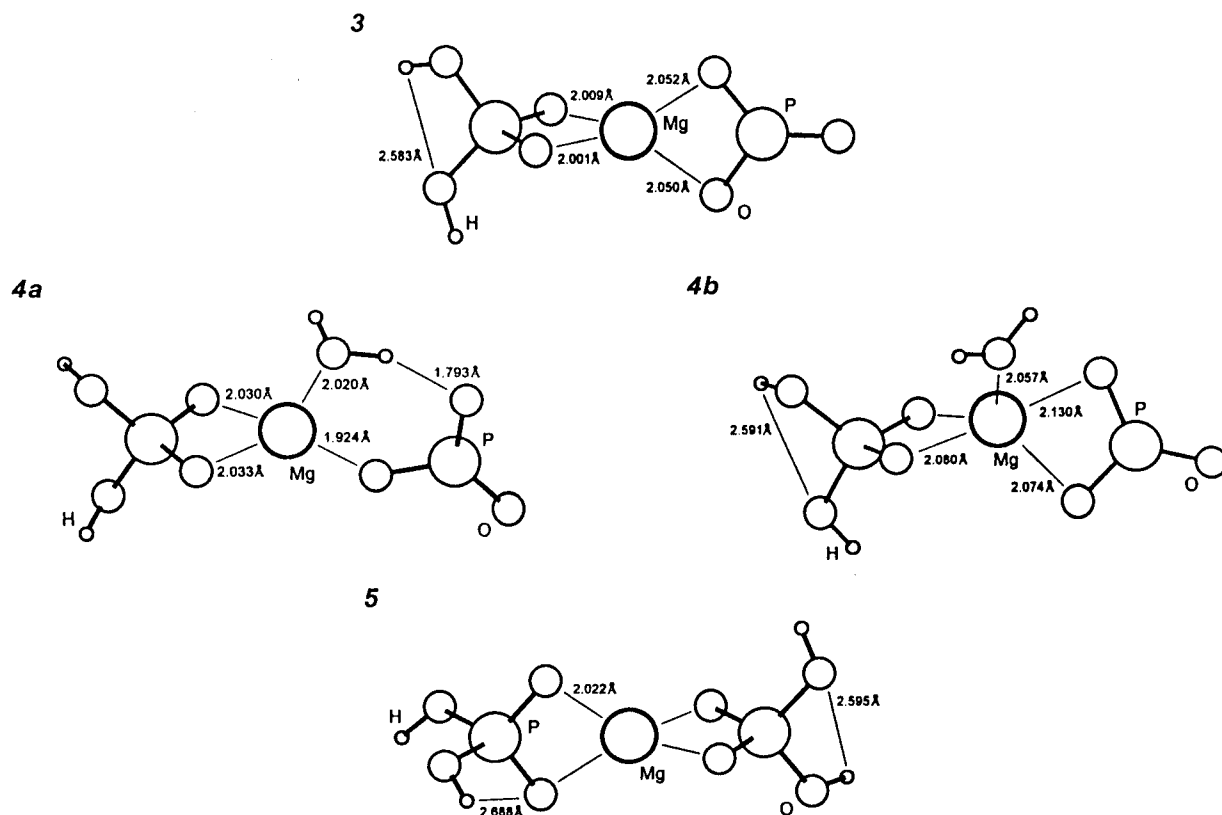


Figure 2. Anhydrous (**3**) and monohydrated (**4a**, **4b**) putative metaphosphate intermediates for the hydrolysis of the neutral Mg–pyrophosphate complex to structure **5**.

phosphate, and the metaphosphate, whose charges were obtained by adding the charges of their corresponding atoms.

Whereas the formal charge of the Mg cation is $+2e$ ($1e = 1.6022 \times 10^{-19}$ C is the elementary charge), it can be seen in Table 3 that in complexes **1a** and **1b** the corresponding Mulliken's charge is less than $+1e$. This small value reflects an electron-rich environment provided by the oxygens that are coordinated by the cation. The comparison with the Mulliken's charges of structures **2a** and **2b** shows that the water molecule makes a small contribution to the electron density surrounding the Mg cation. Moreover, the water molecule does not produce any sizable effect on the charge distribution of the complex.

On the other hand, the apportionment of charges within the CHELP scheme requires an estimate of the radii of the various atoms in the molecule; this poses a particular problem in the case of Mg because its effective radius depends on its coordination. We decided to perform the CHELP analysis with the ionic radius for a coordination number of 4, $r = 0.71$ Å (for comparison, the charges obtained with the van der Waals radius, $r = 1.70$ Å, are also available³¹). The CHELP charge on the Mg is almost twice that obtained from Mulliken's analysis, but still smaller than $+2e$. There is a small decrease from $+1.73e$ in **1b** to $+1.60e$ in **2b**, and a small increase on the charge of the bridging oxygen, from $-0.87e$ in **1a** to $-0.75e$ in **2a**. Of course, the charge distributions of structures **1a** and **1b** are different, due to the positions of the hydrogens. Though small, the variation of the CHELP charges reflects an effect of the water molecule on the electrostatic potential around the Mg–Ppi complex.

3.1.2. Interaction of $PO_3 \cdot Mg \cdot H_2PO_4$ with One Water Molecule. The global minimum for this complex has been found previously^{15,22} and labeled 2×2 (structure **3**, Figure 2). Using it as a starting point, the interaction with water yields structure **4a** (Figure 2). The water molecule displaces one of the

metaphosphates' oxygens that is now hydrogen bonded to the water molecule, thus bending the P–Mg–P angle from linear to 144° . The Mg^{2+} cation coordinates four oxygens that lie in two O–Mg–O orthogonal planes. In fact, the only atoms out of the P–Mg–P plane are the coordinated oxygens belonging to the orthophosphate moiety and the two hydrogens of the same moiety. The interaction energy with the water molecule is about 43% that of the corresponding Mg–pyrophosphates (Table 2); the isomerization **2a** \rightarrow **4a** is predicted to be thermoneutral and spontaneous, whereas the isomerization **2b** \rightarrow **4a** is endothermic and nonspontaneous (Table 4).

Another stationary point was found (structure **4b**, Figure 2), where the Mg^{2+} cation still coordinates four oxygens of the phosphates, but the oxygen of the water molecule occupies a fifth place in the hydration shell, thus modifying the arrangement of the phosphates, as reflected by the RMS difference of 0.497 Å between the Mg–phosphates complexes of **3** and **4b**. The main structural effects induced by the water molecule are the breaking of the orthogonality of the planes formed by the phosphates' oxygens coordinated by the Mg^{2+} cation, and that the cation is no longer aligned with the P atoms. At the SCF level, structure **4b** has a slightly higher energy than **4a**; nevertheless, at the MP2 level, the situation is reversed so the interaction with the water molecule has an enthalpy of $\Delta H^\circ = -89.6$ kJ/mol, and a free energy of $\Delta G^\circ = -51.8$ kJ/mol, about 46% that of the corresponding Mg–pyrophosphates (Table 2). The isomerizations **2a** \rightarrow **4b** and **2b** \rightarrow **4b** are practically thermoneutral, but both are predicted to be spontaneous (Table 4).

The comparison of the isomerization energies of the anhydrous species with respect to the monohydrated species is presented in Table 4. It can be seen that the large shift toward thermoneutrality is due to a stronger interaction of the water molecule with the reactants than with the products, despite the

TABLE 4: Isomerization Energies, Enthalpies, Entropies, and Free Energies of Mg–Phosphates^a

reaction	ΔE_c^{SCF}	ΔE_c^{MP2}	$\Delta E_{\text{th}}^{298}$	ΔH°	ΔS°	ΔG°	$\Delta\Delta G_{\text{sol}}$	ΔG_{aq}
1a → 3^b	−48.1	−6.3	−1.3	−55.6	49.8	−70.4	52.3	18.1
1b → 3	−31.4	−18.3	−3.4	−53.1	37.0	−64.1	66.6	2.5
2a → 4a	3.7	−2.0	−1.1	0.6	35.6	−10.0	46.4	36.4
2b → 4a	22.7	−13.8	−0.6	8.3	14.7	3.9	41.0	44.9
2a → 4b	8.1	−13.0	−1.2	−6.1	36.8	−17.1	39.8	22.7
2b → 4b	27.1	−24.9	−0.7	1.6	15.9	−3.1	34.4	31.3
6b → 8	−15.8	−8.6	0.4	−24.0	52.3	−39.6	31.5	−8.1
7 → 9	11.3	−0.7	0.9	11.6	55.4	−4.9	27.4	22.5
11a → 13a^b	29.7	−9.2	−3.3	17.2	31.8	7.7	56.2	63.9
11b → 13b	14.4	11.1	0.0	25.5	78.2	2.2	−30.5	−28.3
12a → 14a	49.3	−16.5	−3.7	29.1	55.5	12.6	69.4	82.0
12b → 14b	115.1	−3.3	−4.9	106.9	80.6	82.9	0.7	83.6

^a All energies and enthalpies are in kJ/mol. Entropies are in J/(mol K). The last two columns are the differences in solvation free energy and the free energies in aqueous solution, computed with PCM.³³ ^b Data taken from ref 15.

TABLE 5: Hydrolysis Energies, Enthalpies, Entropies, and Free Energies of Monohydrated Mg–Pyrophosphates^a

reaction	ΔE_c^{SCF}	ΔE_c^{MP2}	$\Delta E_{\text{th}}^{298}$	ΔH°	ΔS°	ΔG°	$\Delta\Delta G_{\text{sol}}$	ΔG_{aq}
2b → 5	−94.7	18.4	−0.4	−76.7	−11.8	−73.2	24.7	−48.5
7 → 10	−81.1	30.1	−2.3	−53.3	31.5	−62.7	22.6	−40.1
12a → 15	−252.5	38.6	−1.3	−215.2	9.3	−217.9	73.8	−144.1
12b → 15	−13.1	16.4	−0.4	2.9	24.3	−4.4	−22.0	−26.4

^a All energies and enthalpies are in kJ/mol. Entropies are in J/(mol K). The last two columns are the differences in solvation free energy and the free energies in aqueous solution, computed with PCM.³³

decrease in entropy (Table 2). At a first glimpse, this behavior seems counterintuitive and requires a more careful analysis: the product **4a** not only preserves four oxygens in the first hydration shell of the metal cation, but the water molecule also establishes a hydrogen bond with one oxygen of the metaphosphate moiety; the product **4b** has five oxygens in the first hydration shell and the protons of the water molecule point toward one oxygen of the phosphate moiety and one of the metaphosphate moiety. Besides, it would be expected that the electrostatic relaxation due to the withdrawal of the H_2PO_4^- moiety from the PO_3^- moiety should contribute to a negative enthalpy. All of this is true, so structures **4a** and **4b** are stable. Nevertheless, it is precisely the enthalpy of the interaction with water that stabilizes the reactants. In fact, the addition of a water molecule to structures **1a** and **1b** increases the amount of oxygens coordinated by the metal cation, whereas structure **3** already has a tight coordination, so the addition of the water molecule produces a larger oxygen–oxygen repulsion, thus disturbing the original array.

The Mulliken charge on the Mg cation in structures **3**, **4a**, and **4b** is smaller than in **1a**, **1b**, **2a**, and **2b** (0.8e vs 1.0e, see Table 3), suggesting a slightly higher electron density around the cation.

3.1.3. The Hydrolysis $\text{H}_2\text{O}\cdot\text{Mg}\cdot\text{H}_2\text{P}_2\text{O}_7 \rightarrow \text{H}_2\text{PO}_4\cdot\text{Mg}\cdot\text{H}_2\text{PO}_4$. The optimal geometry found for the product $\text{H}_2\text{PO}_4\cdot\text{Mg}\cdot\text{H}_2\text{PO}_4$ is a 2×2 structure (**5**, Figure 2): the Mg^{2+} cation is aligned with the phosphorus atoms and coordinates four oxygens, two from each phosphate, forming two O–Mg–O orthogonal planes, quite similar to structure **3**. The hydrolysis is predicted to be both exothermic and spontaneous at room temperature (Table 5). It is likely that the presence of other water molecules will alter this configuration, to fulfill the octahedral coordination properties of the Mg^{2+} cation. A proposal for the pathway of the hydrolysis will be presented at the end of this section.

3.2. Hydrolysis of the Monoanionic Complex $[\text{Mg}\cdot\text{HP}_2\text{O}_7]^-$.
3.2.1. Interaction of $[\text{Mg}\cdot\text{HP}_2\text{O}_7]^-$ with One Water Molecule. The optimum geometry found in previous works^{15,22} is the staggered configuration **6a**, with three oxygens coordinated by the Mg^{2+} cation and a hydrogen bond between the proton and an oxygen of the same moiety (Figure 3). Starting from an

eclipsed configuration, in this work we found another stationary point (structure **6b**) with a lower energy than **6a** ($\Delta E^{\text{SCF}} = -10.9$ kJ/mol). It is a staggered geometry with three oxygens coordinated by the Mg^{2+} cation and a hydrogen bond between the proton of the orthophosphate and an oxygen of the opposite metaphosphate. This interaction induces a bent that places the Mg^{2+} cation outside the plane of the P–O–P bridge. The asymmetry of the electrostatic interactions induced by the cation produces the elongation of one of the bridging P–O bonds with respect to the other. The enthalpy and free energy of **6b** are also lower than those of **6a**: $\Delta H^\circ = -17.0$ kJ/mol and $\Delta G^\circ = -12.5$ kJ/mol. Thus, the interaction with water is studied only for **6b**. It can be seen in Table 1 that the lowest frequencies correspond to the same degrees of freedom as for the neutral complex: the bent between the orthophosphate and the metaphosphate planes around the angle ϕ depicted in Figure 3, and the ball-and-socket joint motion.

The optimum geometry of the $[\text{H}_2\text{O}\cdot\text{Mg}\cdot\text{HP}_2\text{O}_7]^-$ complex is structure **7** (Figure 3). Besides being coordinated by the metal cation, the water molecule forms a hydrogen bond with one oxygen of the pyrophosphate, yielding an interaction enthalpy of $\Delta H^\circ = -115.2$ kJ/mol and a free energy of $\Delta G^\circ = -75.6$ kJ/mol. Little distortion is induced on the $[\text{Mg}\cdot\text{HP}_2\text{O}_7]^-$ complex by the water molecule: the RMS difference is 0.044 Å. It is worthwhile to note that the interaction of the water molecule with the monoanionic complex is 20% weaker than with the neutral complex (see Table 2).

As expected, the Mulliken charge on the Mg cation in structure **6b** is even smaller than in the neutral complexes, due to the excess electron (Table 3). The corresponding CHELP charge shows the same behavior. Again, the effect of the water molecule on both the electron density and on the electrostatic potential of the Mg–PPi complex is only marginal.

3.2.2. Interaction of $[\text{PO}_3\cdot\text{Mg}\cdot\text{HPO}_4]^-$ with One Water Molecule. The optimal geometry of the anhydrous complex is a 2×2 structure^{15,22} (**8**, Figure 4). Though structure **4b** was used as a starting point, the resulting geometry upon interaction with water is more similar to **4a** (structure **9**, Figure 4): the oxygen of the water molecule is coordinated to the Mg^{2+} cation, displacing one of the metaphosphate oxygens that gets hydrogen

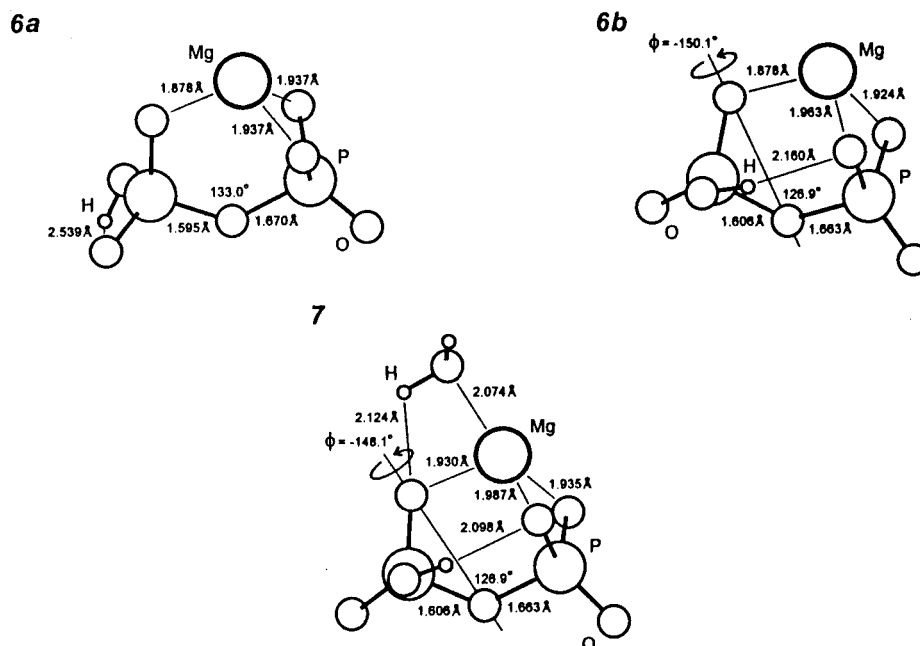


Figure 3. Monoanionic $[\text{Mg}\cdot\text{HP}_2\text{O}_7]^-$ complex. Structure **6a** has been previously reported as optimal^{15,22} but the hydrogen bond in **6b** makes it more stable. Structure **7** results from the interaction with the water molecule. The lowest vibrational frequencies of **6b** and **7** correspond to the bent of the orthophosphate with respect to the dihedral angle ϕ .

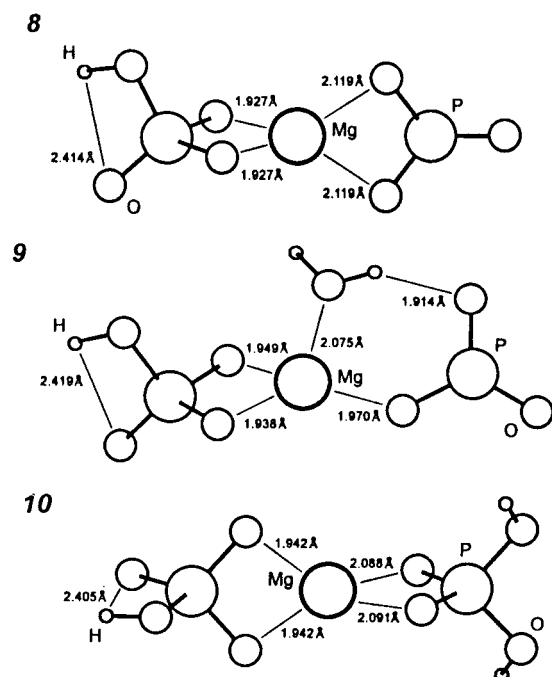


Figure 4. Anhydrous (**8**) and monohydrated (**9**) putative metaphosphate intermediates for the hydrolysis of the monoanionic Mg–pyrophosphate to structure **10**.

bonded to water, causing the loss of orthogonality between the planes formed by the phosphates' oxygens and the disalignment of the Mg^{2+} cation out of the P–P line. The RMS difference between the Mg–phosphates complexes of **8** and **9** is 0.689 Å. The enthalpy of the interaction is $\Delta H^\circ = -79.8$ kJ/mol, and the free energy is $\Delta G^\circ = -40.8$ kJ/mol, about 54% that of the corresponding Mg–pyrophosphate (Table 2). As is the case for the neutral complexes, the interaction with water stabilizes the reactant **7**, thus shifting the enthalpy of the isomerization $7 \rightarrow 9$ to endothermicity, as compared to the exothermicity of $6b \rightarrow 8$ (Table 4). The reasons argued in the previous case also explain

this shift. However, the isomerization $7 \rightarrow 9$ has a negative free energy due to the entropic contribution.

It is interesting to note that the Mulliken charge on the Mg cation is roughly the same in structures **6b**, **7**, and **9**, whereas it is smaller in **8**. This reflects that the high electron density in **8** is lowered by the interaction with the water molecule.

3.2.3. The Hydrolysis $[\text{H}_2\text{O}\cdot\text{Mg}\cdot\text{HP}_2\text{O}_7]^- \rightarrow [\text{H}_2\text{PO}_4\cdot\text{Mg}\cdot\text{HPO}_4]^-$. The product of this hydrolysis is also a 2×2 structure (**10**, Figure 4), with the same features as **5**. In fact the RMS difference between them is of 0.532 Å, and neglecting the hydrogens it reduces to 0.215 Å. The reaction is also predicted to be exothermic and spontaneous at room temperature (Table 5). The previous remark about configurational changes upon hydration also hold in this case.

3.3. Hydrolysis of the Dianionic Complex $[\text{Mg}\cdot\text{P}_2\text{O}_7]^{2-}$.

3.3.1. Interaction of $[\text{Mg}\cdot\text{P}_2\text{O}_7]^{2-}$ with One Water Molecule. This complex has also been studied previously.^{15,22} Though an eclipsed geometry had been found (**11b**, Figure 5), the staggered configuration **11a** remained as the global minimum at the SCF/6-31+g** level of the theory. However, the contribution of correlation favors the eclipsed geometry by $\Delta E^{\text{SCF}+\text{MP}2} = -4.8$ kJ/mol so that the rotation $11a \rightarrow 11b$ has an enthalpy of $\Delta H^\circ = -5.1$ kJ/mol and a free energy of $\Delta G^\circ = -1.1$ kJ/mol. These values are in the limits of accuracy of the method, so the theoretical prediction is that both structures are equally probable. The staggered configuration has an elongated bridging P–O bond, whereas the eclipsed geometry has D_h symmetry. A study of the rotational barrier will be published elsewhere.²⁷

The normal modes of vibration are presented in Table 1. Whereas the two lowest frequencies of structure **11a** correspond to the bent between the orthophosphate and the metaphosphate planes around the angle ϕ depicted in Figure 5, and the ball-and-socket joint motion, the lowest frequency of structure **11b** is the rotation of the orthophosphate and the metaphosphate around an axis passing through the two phosphorus atoms; the second lowest frequency motion is the bending between the orthophosphate and the metaphosphate planes around an axis passing through the bridging oxygen and the Mg cation, as depicted in Figure 5.

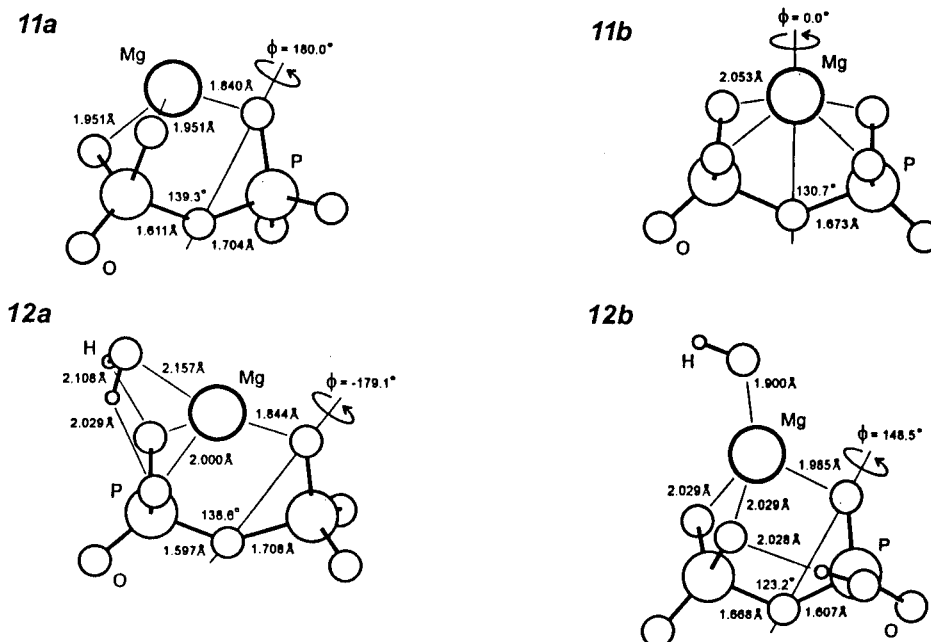


Figure 5. Staggered (**11a**) and eclipsed (**11b**) configurations of the dianionic $[\text{Mg}\cdot\text{P}_2\text{O}_7]^{2-}$ complex. Structures **12a** and **12b** result from the interaction with one water molecule, that is dissociated in the latter configuration. The lowest frequencies of structures **11a**, **12a**, and **12b** correspond to the bent of the orthophosphate moiety with respect to the dihedral angle ϕ , whereas the lowest frequencies of the eclipsed geometry are a rotation of the phosphates around an axis passing through the phosphorus atoms, and the bending of the orthophosphate moiety with respect to an axis passing through the Mg^{2+} and the bridging oxygen. Structure **12b** results very stable.

Starting from structure **11a**, a stationary point for the complex with water was obtained (**12a**, Figure 5). The water molecule forms two hydrogen bonds with the oxygens of the pyrophosphate. The interaction enthalpy and free energy are $\Delta H^\circ = -121.7$ kJ/mol and $\Delta G^\circ = -81.5$ kJ/mol. The RMS difference between the Mg–pyrophosphates of structures **11a** and **12a** is of 0.034 Å, showing little distortion induced by the water molecule. The interaction of the water molecule with the dianionic complex has an energy similar to the interaction with the monoanionic complex (Table 2). The two lowest frequencies correspond to the same degrees of freedom as in structure **11a**. Moreover, the values remain practically unchanged (Table 1).

Because this Mg–PPi complex is completely deprotonated, the excess electrons are more easily displaced by the water molecule. This is reflected in a larger change induced on the charges assigned to the various moieties of the complex than in the previous cases.

On the other hand, when structure **11b** was used as the starting point, the water molecule readily broke and the resulting staggered structure **12b** is a complex $[\text{OH}\cdot\text{Mg}\cdot\text{HP}_2\text{O}_7]^{2-}$ that has a much lower energy than the complex with water (**12a** ($\Delta G^\circ = -213.3$ kJ/mol)). The reaction of a water molecule with Mg–pyrophosphate in structure **11b** to structure **12b** has an enthalpy of $\Delta H^\circ = -334.5$ kJ/mol and a free energy of $\Delta G^\circ = -293.7$ kJ/mol. A hydrogen bond is formed by one oxygen of the pyrophosphate with the hydrogen at the opposite moiety. The formation of a hydroxide ion seems consistent with the mechanism proposed by Heikinheimo et al.²¹ for the hydrolysis in the catalytic site of yeast inorganic pyrophosphatase. Nevertheless, to make the nucleophilic attack, the OH^- anion should migrate from the coordination sphere of the metal cation. On the other hand, structure **12b** can also be seen as a $[\text{Mg}\cdot\text{HP}_2\text{O}_7]^-$ complex interacting with the hydroxide; the estimates of the enthalpy and free energy can be obtained from comparison to **6b** + $\text{OH}^- \rightarrow \text{12b}$ and result quite favorable: $\Delta H^\circ = -198.8$ kJ/mol and $\Delta G^\circ = -161.7$ kJ/mol; even more favorable than the interaction of **6b** with water. This unexpected result amounts

to saying that the theoretical prediction of the species in aqueous solution might not be the hydrated complex $[\text{Mg}\cdot\text{P}_2\text{O}_7]^{2-}$, but the hydrated $[\text{OH}\cdot\text{Mg}\cdot\text{HP}_2\text{O}_7]^{2-}$ complex. However, in aqueous solution the interaction energy of the Mg–PPi monoanion with hydroxide should easily be paid for by the hydration of both ions, and thus the effect would be to release hydroxides to the solution, where they would capture protons and increase the pH. This is opposite to pH measurements of aqueous solutions of pyrophosphate to which MgCl_2 is added: the pH decreases to a value corresponding to the release of two protons from the diphosphoric acid upon formation of the Mg–PPi complex.³² This disagreement could be attributed to the effects of using a small basis set, or to a deficient level of the theory to include correlation energy; but previous calculations have shown that neither is the case.²² Therefore, what can be said from the theoretical result is that there is a minimum number, as yet undetermined, of water molecules hydrating the dianionic Mg–PPi complex needed to prevent the formation of a hydroxide anion. The possible implications of this result on the proposal of the mechanism of hydrolysis will be discussed at the end of this section.

3.3.2. Interaction of $[\text{PO}_3\cdot\text{Mg}\cdot\text{PO}_4]^{2-}$ with One Water Molecule. For this complex, the optimal geometry has been labeled^{15,22} 3 × 1 (**13a**, Figure 6). In this work another stationary point was found (structure **13b**, Figure 6) that has a slightly lower energy than the former ($\Delta H^\circ = 3.5$ kJ/mol and $\Delta G^\circ = -6.4$ kJ/mol). Because these values are in the limits of accuracy of the calculations, structures **13a** and **13b** should be considered isoenergetic. In the same scheme of labeling, this new geometry is a 2 × 1 configuration. There are only three oxygens coordinated by the metal cation, at shorter distances than in **11b**.

The interaction of **13a** with water yields structure **14a**, that has the Mg^{2+} cation disaligned from the P–P line, and coordinating five oxygens: three from the PO_4 moiety, one from PO_3 , and one from the water molecule, this latter being 0.3 Å further from the cation than the other oxygens. The RMS

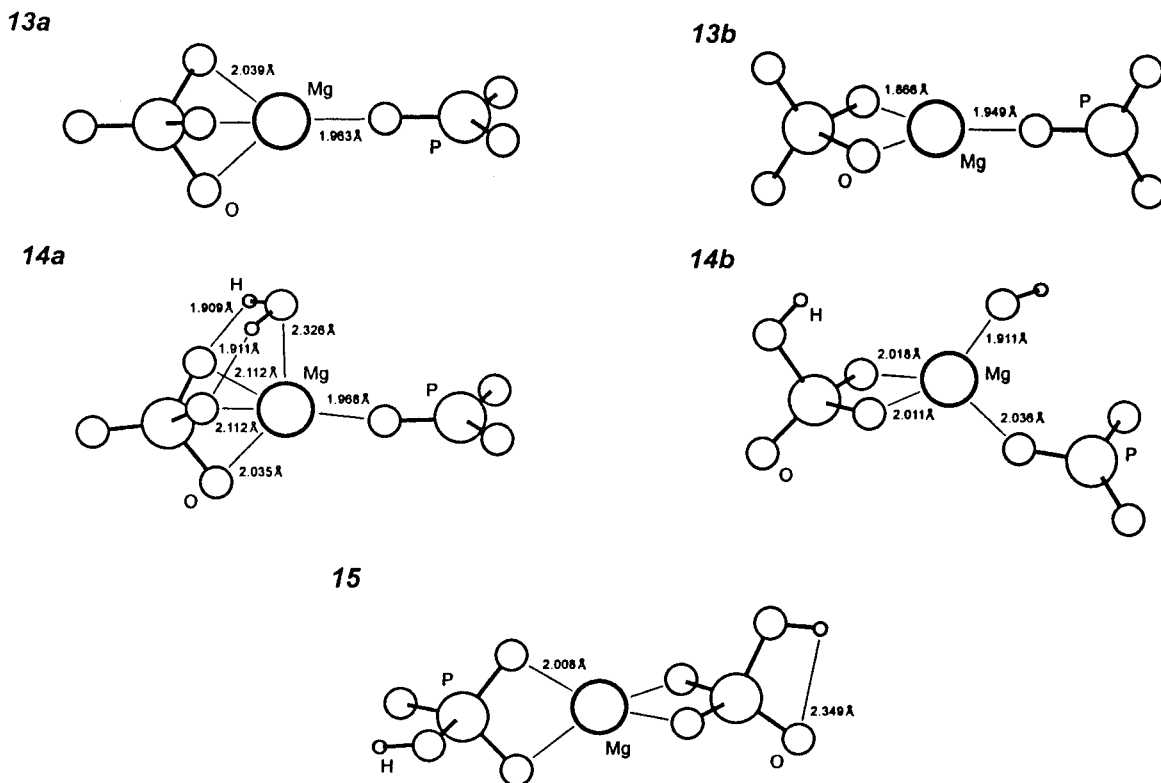


Figure 6. Structure **13a** has been previously reported as having the global energy minimum of the metaphosphate isomer of the dianionic Mg–pyrophosphate complex. Structure **13b** is practically isoenergetic to **13a**. Structures **14a** and **14b** result from the interaction with one water molecule, that is dissociated in the latter configuration. Structure **14b** has a substantially lower energy than **14a**, but it is still higher than that of structure **12b**. Moreover, the product of the hydrolysis **15** is practically isoenergetic with **12b**.

difference between the Mg–phosphates complexes of **13a** and **14a** is 0.149 Å. The water molecule forms two hydrogen bonds with the PO_4 moiety and interacts with the $[\text{PO}_3\cdot\text{Mg}\cdot\text{PO}_4]^{2-}$ complex with an enthalpy of $\Delta H^\circ = -111.5$ kJ/mol, and a free energy of $\Delta G^\circ = -80.0$ kJ/mol; both the enthalpy and the free energy are nearly the same as for the interaction of **11a** with water (Table 2). Starting from **13b** leads to structure **14b** (Figure 6), in which the water molecule breaks into a proton and a hydroxide anion. The reaction of the water molecule with **13b** to produce **14b** has an enthalpy of $\Delta H^\circ = -253.1$ kJ/mol and a free energy of $\Delta G^\circ = -213.0$ kJ/mol, whereas the reaction **12b** \rightarrow **14b** is endothermic and nonspontaneous (Table 4). The large positive free energy can be attributed to the existence in **14b** of three negatively charged species (Table 5) that repel each other: the CHELP charge on hydroxide is $-0.9e$, on the orthophosphate is $-1.9e$, and on the metaphosphate is $-1.0e$, as compared to **12b** where the charge on the hydroxide is $-1.0e$ and on the HP_2O_7 moiety is $-2.8e$; other features that stabilize **12b** are the chemical bond that makes the pyrophosphate, and the hydrogen bond between the orthophosphate and the metaphosphate.

Analogously to the case of **12b**, **14b** can be seen as the interaction of **8** with the hydroxide anion, and the interaction energy obtained from $\mathbf{8} + \text{OH}^- \rightarrow \mathbf{14b}$: $\Delta H^\circ = -67.0$ kJ/mol and $\Delta G^\circ = -38.1$ kJ/mol. Opposite to the case of the Mg–pyrophosphate, the interaction with the hydroxide ion is weaker than with the water molecule (Table 2). The consequences of this result on the proposal of the pathway for the hydrolysis of Mg–pyrophosphate in aqueous solution will be discussed at the end of this section.

3.3.3. The Hydrolysis $[\text{H}_2\text{O}\cdot\text{Mg}\cdot\text{P}_2\text{O}_7]^{2-} \rightarrow [\text{HPO}_4\cdot\text{Mg}\cdot\text{HPO}_4]^{2-}$. Structure **15** (Figure 6) is also a 2×2 geometry, very similar to **5** and **10**; however, the RMS difference with **10**

is large, 0.848 Å (0.784 Å, neglecting the hydrogens), due to the different distortion induced on the phosphates by the coordination to the metal cation. The reaction **12a** \rightarrow **15** has a very favorable enthalpy, $\Delta H^\circ = -215.2$ kJ/mol, and free energy $\Delta G^\circ = -217.9$ kJ/mol. However, the reaction **12b** \rightarrow **15** is close to thermoneutral, though spontaneous (Table 5). In fact, the values of enthalpy and free energy are in the limits of accuracy, so the prediction at this level of the theory is that structures **12b** and **15** are isoenergetic.

3.4. Effect of Solvation. Once the stationary states of the gas phase have been determined, it is worth studying the effect of the aqueous environment on their relative stabilities. A simple way to do this is by means of continuum solvation methods that provide an estimate of the solvation free energies. In this work we applied the polarizable continuum model of Tomasi (PCM³³), using a dielectric constant of 78.390 and a grid of 200 points. The solvation energies ΔG_{sol} obtained for each complex are shown in the last column of Table 3, whereas the last two columns of Tables 4 and 5 show the differences in solvation energies $\Delta\Delta G_{\text{sol}}$ and the predicted free energies of the proposed reactions in aqueous solution ΔG_{aq} . In general terms, solvation stabilizes the pyrophosphates relative to the complexes with metaphosphate and to the products of hydrolysis, exception made of the dianionic structures **11b** and **12b**. As a consequence, the free energies of the hydrolysis reactions in Table 5 reach values similar to those reported by George et al.²⁸ from calorimetric measurements in aqueous solution: $\Delta G^\circ = -39.7$ kJ/mol for $\text{H}_4\text{P}_2\text{O}_7$, $\Delta G^\circ = -31.4$ kJ/mol for $\text{H}_3\text{P}_2\text{O}_7^-$, $\Delta G^\circ = -32.2$ kJ/mol for $\text{H}_2\text{P}_2\text{O}_7^{2-}$, $\Delta G^\circ = -29.7$ kJ/mol for $\text{HP}_2\text{O}_7^{3-}$, and $\Delta G^\circ = -43.5$ kJ/mol for $\text{P}_2\text{O}_7^{4-}$. Direct comparison is, however, not possible because the reactions reported by them do not consider the complexes with the metal cation, and because the results in this work refer to the product

orthophosphates coordinated by one magnesium. Nevertheless, the agreement does not seem to be merely coincidental, but a result of taking into account the interaction with the solvent.

4. Discussion

From the results in the previous section, a general picture can be obtained that has some implications on the mechanism of the hydrolysis of pyrophosphate in the active site of enzymes: it is worth noticing that the interactions with the water molecule are all characterized by a large enthalpy and a large decrease in entropy (Table 2). This reflects mainly the strong interaction with the metal cation as well as the restriction imposed by its coordination properties on the positions attainable by the water molecule. In the hydrolysis reactions, both the enthalpies and the free energies are also determined mainly by the SCF energies (Table 5), whereas the free energies of the isomerizations depend to a large extent on the favorable changes in entropy that counteract unfavorable enthalpies in various instances (Table 4). The data presented in Tables 2, 4, and 5 were obtained from standard statistical mechanics²⁵ applied to the harmonic frequencies computed from second derivatives of the energies. Typically, a scaling factor of 0.9 is applied to the theoretical frequencies²⁵ when using the 6-31+G** basis set. This scaling would affect the thermal energy $\Delta E_{\text{ther}}^{298}$ and the vibrational contribution to the entropy, that are a small percentage of the total enthalpy and entropy; nevertheless, to assess a quantitative estimate of the accuracy of our calculations, we computed the vibrational contributions with scaling factors of 0.9 and 1.1 on the frequencies. The total effect on the free energies is less than ± 5 kJ/mol in all cases. Therefore, the qualitative conclusions for the interactions with the water molecule and with the hydroxide anion are not modified, and the comparison of both the isomerizations to metaphosphate intermediates and the hydrolyses shows that the interaction with one water molecule stabilizes the Mg-pyrophosphates. This is corroborated by the estimates of the free energies of solvation made with the polarizable continuum model.

The hydrolyses of the monohydrated neutral and monoanionic species are predicted to be exothermic and spontaneous, whereas the hydrolysis of the dianionic species $[\text{HO}\cdot\text{Mg}\cdot\text{HP}_2\text{O}_7]^{2-}$ is practically thermoneutral and reversible. This result is in agreement with some recent theories about the functioning of both PP-ases and ATP-ases.^{34,35} However, when solvation is taken into account, all the hydrolyses become spontaneous and the computed free energies get closer to the experimental values. This supports the proposal made by George et al.²⁸ that the energy made available to the metabolism from the hydrolysis of phosphoanhydride bonds is mainly due to the difference in solvation between reactants and products.

The relative gas-phase energies of the various stable configurations found in this work are depicted in the graphs of Figure 7. The effect of solvation can be seen in the corresponding graphs of Figure 8. This allows a comparison of possible pathways for the hydrolysis reactions of the three ionic species of the Mg-PPi complex studied in this work.

In the gas phase the neutral structures **1a** and **1b** are equally likely, and both interact strongly with the water molecule; however, the isomerization to the metaphosphate intermediates, either the anhydrous **3** or the monohydrated **4b**, seems to require the two protons to be at the orthophosphate moiety so the reaction route has to go through **2a**. The most stable monohydrated metaphosphate intermediate is **4b**, but it is likely that

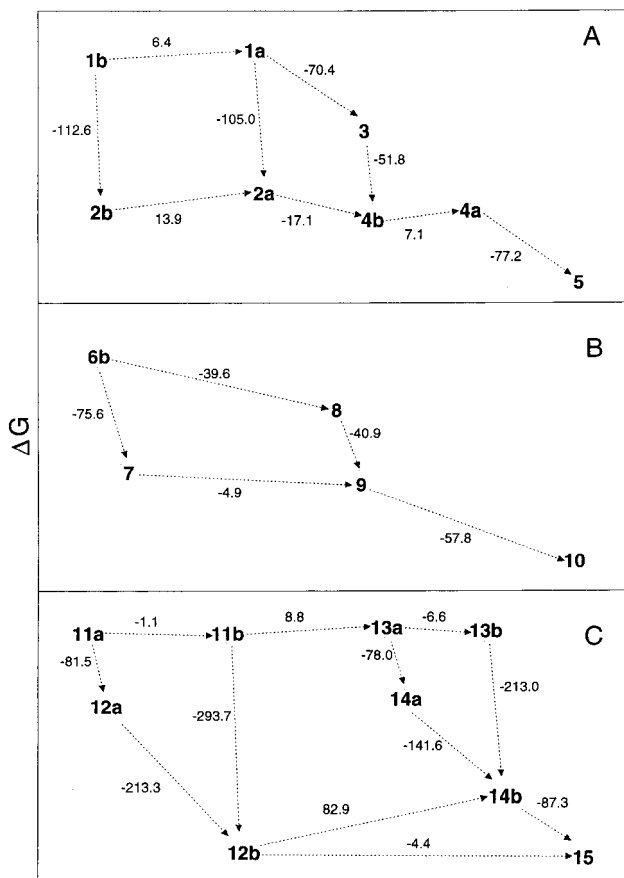


Figure 7. Graphs showing the proposed reaction paths for the neutral (A), monoanionic (B), and dianionic (C) Mg-pyrophosphate complexes. The numbers in boldface correspond to the structures of Figures 1–6. The smaller numbers close to each line correspond to the estimated free energy ΔG from one structure to the other, in kJ/mol.

the more open structure **4a** is a step to full hydrolysis **5**. Though solvation favors structure **1b**, it also reduces the difference between structures **2a** and **2b** and makes the metaphosphate complexes substantially less favorable. It should be kept in mind that all the structures mentioned are stationary states, and further studies are required to analyze the barriers between them; the only transition state that has been reported^{14,15} is that between **1a** and **3**.

In a similar manner, the monoanionic species can be seen as starting from **6b** then interacting with water to yield **7**, undergoing isomerization to **9**, that is already an open structure, and finally hydrolyzing to **10**. Again, solvation hinders the isomerization to a metaphosphate intermediate.

The case of the dianionic Mg-PPi is far more complicated due to the various possibilities of hydrogen-bonding, that lead to the unexpected result of breaking the water molecule into a proton that binds to the pyrophosphate and a hydroxide anion that gets coordinated by the metal cation. The very large free energy of this reaction makes the route through structure **12b** the most likely by far. The metaphosphate intermediate should then be structure **14b** from which the hydrolysis proceeds to completion to **15**. However, the isomerization **12b** \rightarrow **14b** is quite unfavorable, with a free energy of $\Delta G^\circ = 82.9$ kJ/mol, whereas the hydrolysis **12b** \rightarrow **15** is practically thermoneutral and reversible. Opposite to the previous cases, solvation favors the hydrolysis of the dianionic pyrophosphate; but it preserves the positive free energy of **14b** relative to **12b**, and the latter is still predicted to be more stable than **12a**. This seems to support an associative mechanism for the hydrolysis through the

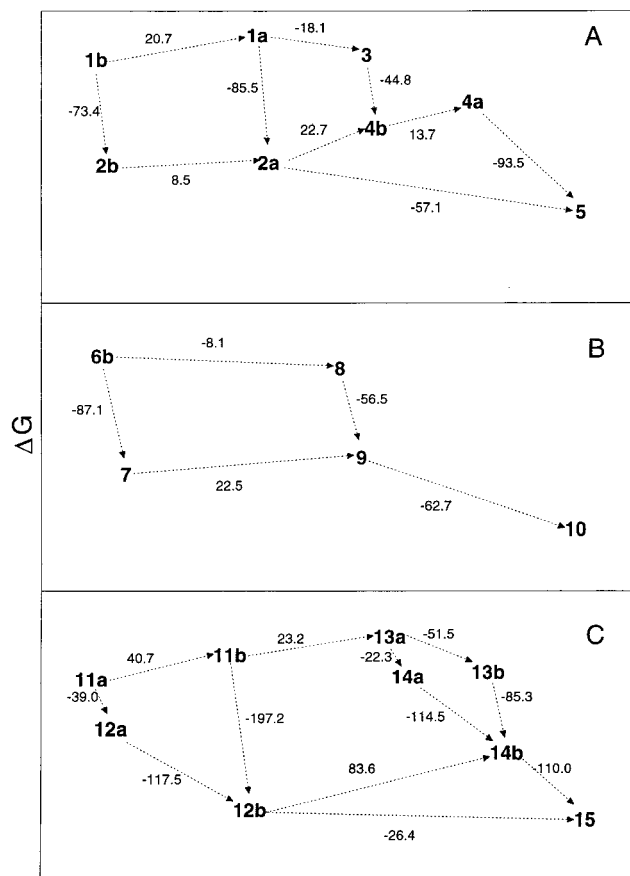


Figure 8. Graphs showing the effect of solvation on the proposed reaction paths for the neutral (A), monoanionic (B), and dianionic (C) Mg–pyrophosphate complexes. See caption of Figure 7.

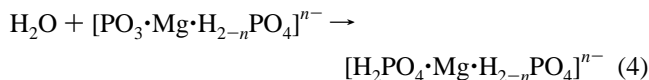
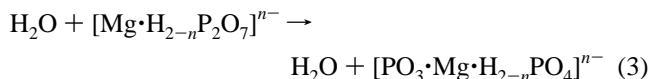
nucleophilic attack of the OH^- anion on one of the phosphorus atoms.^{37,38} Nevertheless, it is not yet possible to assess the energetic cost of displacing the OH^- anion from the coordination sphere of the metal cation and then perform the nucleophilic attack. Further studies are required that include more explicit water molecules.

On the other hand, the result of the dissociation of the water molecule does not discard the possibility of a dissociative mechanism for the hydrolysis of pyrophosphate in the active site; though there is still disagreement about the number of metal cations within the active site of pyrophosphatases, it is generally accepted that two metal cations take part in the process of hydrolysis.^{13,21,36,39,40} Moreover, X-ray structural data show the presence of a substantial amount of water molecules within the active site.²¹ If structure **12b** were stable upon hydration, it would be the species entering the active site where the second metal cation could attract the hydroxide anion, that would be substituted by a water molecule, thus converting the dianionic **12b** into the monoanionic **7** that can isomerize to **9**. The resulting metaphosphate could be captured by the second metal cation, thus be brought near the hydroxide anion that would perform the nucleophilic attack resulting in the second orthophosphate. Of course, further studies are needed to explore the feasibility of this speculative mechanism, that could also explain the reverse process, i.e., the synthesis.

5. Concluding Remarks

In this work we have studied the equilibrium geometries of monohydrated Mg–pyrophosphate and Mg–phosphate complexes, to compare the dissociative mechanism for the hydrolysis

with a metaphosphate intermediate:¹⁴



where $n = 0, 1, 2$, to the associative mechanism that requires a hydroxide anion as a suitable nucleophile.^{21,37} Previously reported results^{14,15,22} support the dissociative scheme, whereas a recent study³⁸ concludes that the associative scheme is equally likely for the hydrolyses of phosphate esters. In all these studies the interaction with the explicit water molecule is neglected. However, here we found it to be large and distinctly different with the various isomers, so it affects the energetics of the hydrolysis reactions by stabilizing the Mg–pyrophosphate complexes. Moreover, an estimate of the hydration free energies corroborates this conclusion.

In the case of the dianionic complex the water molecule readily dissociates upon interacting with the complex, yielding the hydroxide anion that may act as a nucleophile. Even though this result is consistent with an associative mechanism, it does not discard the dissociative mechanism. To elucidate between both proposals, further studies are needed, that include explicit water molecules.

Acknowledgment. This research was supported by DGAPA-UNAM under Grant IN112896 and by CONACyT under Grant L004-E. Part of the calculations were performed with the computer facilities of Supercómputo, DGSCA-UNAM. We thank Prof. Iván Ortega Blake for fruitful discussion.

Supporting Information Available. Tables listing the Cartesian coordinates of all the structures shown in this paper, referred to their respective PMI frames, with their SCF/6-31+G**, MP2/6-31+G** energies, vibrational frequencies, charges from Mulliken's population analysis, and charges computed with the CHELP scheme with two different radii for the metal cation.³¹ This material is available free of charge via the Internet at <http://pubs.acs.org>.

References and Notes

- (1) Stryer, L. *Biochemistry*; W. H. Freeman and Co.: New York, 1991; pp 316, 456.
- (2) Kraut, J. *Science* **1988**, *242*, 533–540.
- (3) Liu, C.-L.; Hart, N.; Peck, H. D. *Science* **1982**, *217*, 363–364.
- (4) Shakhov, Y. A.; Nyrén, P.; Baltscheffsky, M. *FEBS Lett.* **1982**, *146*, 177–180.
- (5) Baltscheffsky, M.; Nyrén, P. In *Bioenergetics*; Ernster, E., Ed.; Elsevier Science Publishers, B. V.: Amsterdam, 1984; Chapter 6, pp 187–206.
- (6) Saint-Martin, H.; Ortega-Blake, I.; Leś, A.; Adamowicz, L. *Biochim. Biophys. Acta* **1991**, *1080*, 205–214.
- (7) Ma, B.; Meredith, C.; Schaefer, H. F., III. *J. Phys. Chem.* **1994**, *98*, 8216–8223.
- (8) Colvin, M. E.; Evleth, E.; Akacem, Y. *J. Am. Chem. Soc.* **1995**, *117*, 4357–4362.
- (9) Celis, H.; Romero, I. *J. Bioenerg. Biomembr.* **1987**, *19*, 255–272.
- (10) Knight, W. B.; Fitts, S. W.; Dunaway-Mariano, D. *Biochemistry* **1981**, *20*, 4079–4086.
- (11) Ting, S. J.; Dunaway-Mariano, D. *FEBS Lett.* **1984**, *165*, 251–253.
- (12) Shorter, A. L.; Haromy, T. P.; Scalzo-Brush, T.; Knight, W. B.; Dunaway-Mariano, D.; Sundaralingham, M. *Biochemistry* **1987**, *26*, 2060–2066.
- (13) Geue, R. J.; Sargeson, A. M.; Wijsekera, R. *Aust. J. Chem.* **1993**, *46*, 1021–1040.
- (14) Ma, B.; Meredith, C.; Schaefer, H. F., III. *J. Phys. Chem.* **1995**, *99*, 3815–3822.

- (15) Saint-Martin, H.; Ruiz-Vicent, L. E.; Ramírez-Solís, A.; Ortega-Blake, I. *J. Am. Chem. Soc.* **1996**, *118*, 12167–12173.
- (16) De Meis, L. *Biochim. Biophys. Acta* **1989**, *923*, 333–349.
- (17) De Meis, L. *Arch. Biochem. Biophys.* **1993**, *306*, 287–296.
- (18) Saint-Martin, H.; Ortega-Blake, I.; Leś, A.; Adamowicz, L. *Biochim. Biophys. Acta* **1994**, *1207*, 12–23, and references therein.
- (19) Dewar, M. J. S.; Storch, D. M. *Proc. Natl. Acad. Sci. U.S.A.* **1985**, *82*, 2225–2229.
- (20) Warshel, A.; Åqvist, J.; Creighton, S. *Proc. Natl. Acad. Sci. U.S.A.* **1989**, *86*, 5820–5824.
- (21) Heikinheimo, P.; Lehtonen, J.; Baykov, A.; Lahti, R.; Cooperman, B. S.; Goldman, A. *Structure* **1996**, *4*, 1491–1508.
- (22) McCarthy, W. J.; Smith, D. A. M.; Adamowicz, L.; Saint-Martin, H.; Ortega-Blake, I. *J. Am. Chem. Soc.* **1998**, *120*, 6113–6120.
- (23) McCarthy, W. J.; Adamowicz, L.; Saint-Martin, H.; Ortega-Blake, I. *J. Am. Chem. Soc.*, submitted.
- (24) Frisch, M. J.; Trucks, G. W.; Schlegel, H. B.; Gill, P. M. W.; Johnson, B. G.; Robb, M. A.; Cheeseman, J. R.; Keith, T.; Petersson, G. A.; Montgomery, J. A.; Raghavachari, K.; Al-Laham, M. A.; Zakrzewski, V. G.; Ortiz, J. V.; Foresman, J. B.; Cioslowski, J.; Stefanov, B. B.; Nanayakkara, A.; Challacombe, M.; Peng, C. Y.; Ayala, P. Y.; Chen, W.; Wong, M. W.; Andres, J. L.; Replogle, E. S.; Gomperts, R.; Martin, R. L.; Fox, D. J.; Binkley, J. S.; Defrees, D. J.; Baker, J.; Stewart, J. P.; Head-Gordon, M.; Gonzalez, C.; Pople, J. A. *Gaussian 94*, Revision C.3; Gaussian, Inc.: Pittsburgh, PA, 1995.
- (25) Hehre, W. J.; Radom, L.; v. R. Schleyer, P.; Pople, J. A. *Ab Initio Molecular Orbital Theory*; John Wiley & Sons: New York, 1986; pp 25, 86, 226, 253.
- (26) Bernal-Uruchurtu, M. I.; Ortega-Blake, I. *J. Chem. Phys.* **1995**, *103*, 1588–1598.
- (27) Saint-Martin, H.; Vicent, L. E. *J. Mol. Struct. (THEOCHEM)*, submitted.
- (28) George, P.; Witonski, R. J.; Trachtman, M.; Wu, C.; Dorwart, W.; Richman, L.; Richman, W.; Shurayh, F.; Lentz, B. *Biochim. Biophys. Acta* **1970**, *223*, 1–15.
- (29) Mulliken, R. S. *J. Chem. Phys.* **1955**, *23*, 1833–1840.
- (30) Chirlian, L. E.; Francl, M. M. *J. Comput. Chem.* **1987**, *8*, 894–.
- (31) Saint-Martin, H. Technical Report BP-01-98, 1998, Centro de Ciencias Físicas, UNAM. Available upon request via e-mail: humberto@fis.unam.mx.
- (32) Celis, H. Unpublished results.
- (33) Cossi, M.; Barone, V.; Cammi, R.; Tomasi, J. *Chem. Phys. Lett.* **1996**, *255*, 327–335.
- (34) Blyumenfel'd, L. A.; Tikhonov, A. N. *Biophysics* **1987**, *32*, 865–880 (from *Biofizika* **1987**, *32*, 800–817, printed in Poland).
- (35) De Meis, L. *Arch. Biochem. Biophys.* **1993**, *306*, 287–296.
- (36) Baykov, A. A.; Shestakov, A. S. *Eur. J. Biochem.* **1992**, *206*, 463–470.
- (37) Florián, I.; Warshel, A. *J. Am. Chem. Soc.* **1997**, *119*, 5473–5474.
- (38) Florián, I.; Warshel, A. *J. Phys. Chem. B* **1998**, *102*, 719–734.
- (39) Leigh, R. A.; Pope, A. J.; Jennings, I. R.; Sanders, D. *Plant Physiol.* **1992**, *100*, 1698–1705.
- (40) Sosa, A.; Ordaz, H.; Romero, I.; Celis, H. *Biochem. J.* **1992**, *283*, 561–566.